

DOI 10.24425/ae.2019.129336

Calculation of inductances and induced currents in cryogenic by-pass line for SIS100 particle accelerator at FAIR

ŁUKASZ TOMKÓW^{1,2}, STANISŁAW TROJANOWSKI³, MARIAN CISZEK^{1,3},
MACIEJ CHOROWSKI¹

¹ *Wrocław University of Technology
wyb. Wyspiańskiego 27, 50-370 Wrocław, Poland*

² *Joint Institute for Nuclear Research
Joliot-Curie 6, 141980 Dubna, Russia*

³ *Institute of Low Temperature and Structure Research
ul. Okólna 2, 50-422 Wrocław, Poland
email: lukasz.tomkow@pwr.edu.pl*

(Received: 08.11.2018, revised: 20.02.2019)

Abstract: Quality of electric current delivered to the magnets of a particle accelerator is essential for safety and reliability of its operation. Even small discrepancies strongly affect the properties of particle beams. One of the sources of the disturbances is the appearance of induced currents caused by the electromagnetic interactions between the elements of the machine. In this paper the calculations of induced currents in by-pass lines of a SIS100 particle accelerator are presented. In order to find the values of the currents the self-inductances and mutual inductances of the by-pass lines are found. Due to the complex geometry of the line, especially of Ω -shaped dilatations, the numerical approach was employed. The calculations show that the size of induced currents increases with the distance between the cables in an individual bus-bar. The maximum discrepancy of the magnetic field in a dipole magnet is found to be $7.7 \mu\text{T}$. The decrease of distance between the cables allows one to obtain a discrepancy of $1.2 \mu\text{T}$.

Key words: line inductance, mutual inductance, induced currents, superconducting bus-bars, particle accelerators



© 2019. The Author(s). This is an open-access article distributed under the terms of the Creative Commons Attribution-NonCommercial-NoDerivatives License (CC BY-NC-ND 4.0, <https://creativecommons.org/licenses/by-nc-nd/4.0/>), which permits use, distribution, and reproduction in any medium, provided that the Article is properly cited, the use is non-commercial, and no modifications or adaptations are made.

1. Introduction

Interactions between the elements of an electrical circuit can lead to the appearance of induced currents. In the case of particle accelerators their presence is undesired, as they cause the deviation from the required current supplied to the magnets [1]. It leads to the changes of a magnetic field which strength has to be closely synchronized with the parameters of the particle beam in order to avoid beam loss or damage to the beam pipes or the superconducting magnets [2]. Even small discrepancies of the field can divert the particle beam from its desired trajectory. In the case of the magnets for SIS100 the allowed divergence from the nominal field is $6.25 \mu\text{T}$.

Facility for Antiproton and Ion Research, one of the largest modern accelerators, is currently under construction in GSI [3]. The accelerator will consist of 6 cryogenically cooled sections containing superconducting magnets that will be connected with by-pass lines [4]. The by-pass lines are designed at Wrocław University of Technology as the part of Polish in-kind contribution to the FAIR project.

This paper describes the numerical calculations of the values of inductances present in the by-pass lines. Then they are used to find induced currents and estimate the magnetic field discrepancy, which may affect the movement of particles in the beam line. Analytical calculations on this subject along with some experimental measurements were described in [5]. The experimental and numerical analysis of capacitance of the by-pass line is presented at [6].

2. Methods

2.1. Analyzed system

The analysed system is the assembly of four superconducting bus-bars localized within the cryostat of the by-pass line. The typical cross-section of the line is presented in Figure 1. The bus-bars are placed in the corners of a rectangular arrangement. In the final design the pairs of cables are arranged so the pairs in the nearest corner are rotated by 90° with respect to each other. In this paper the analysis of the effect of other placement is analysed and presented. The other lines seen in the figure are process pipes used to carry the cryogenic fluids cooling down the magnets and a thermal shield. All pipes are made of non-magnetic steel [7] provides an elaborate description of a bus-bar and the analysis of its thermal behaviour.

Each bus-bar consists of two superconducting Nuclotron-type cables with NbTi surrounded by a steel tube. The pairs of bus-bars supply with current different types of magnets – dipoles (D in Figure 1), defocusing quadrupoles (DQ) and two groups of focusing quadrupoles (FQ1 and FQ2). The magnets are connected in series, therefore the total inductance of a group is the sum of inductances of the individual magnets. The characteristics of the groups of magnets are gathered in Table 1. The maximum current delivered to the dipole magnets is 13090 A and to the quadrupole magnets – 10874.

The by-pass lines consist of sections with the length of 12.9 m. Bus-bars in each section are equipped with Ω -shaped dilatations to counter the effects of thermal contraction. The dimensions of the dilatations are shown in Figure 2. The dilatations are located on the planes connecting D-FQ1 and FQ2-DQ bus-bar pairs, parallel to each other. The bus-bars are twisted, so the bended

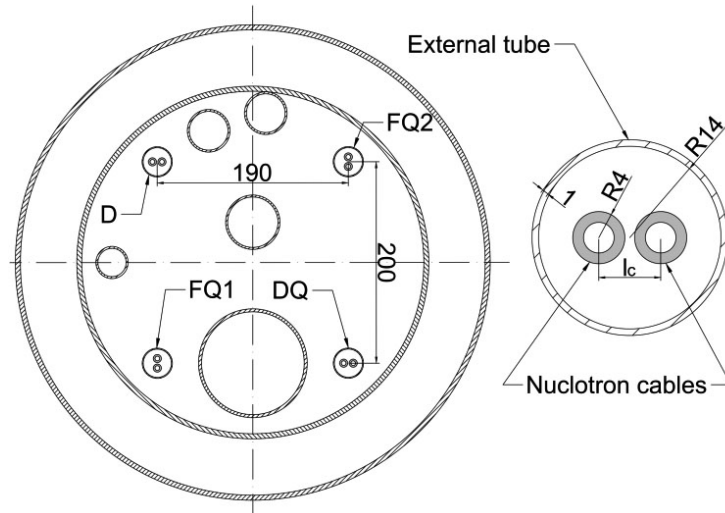


Fig. 1. Cross-section of the cryogenic by-pass line and a single superconducting bus-bar

Table 1. Characteristics of superconducting magnets at FAIR

Magnet	Self-inductance of a single magnet	Number	Total self-inductance	Maximum current
Unit	μH	–	mH	A
Dipole (D)	553	108	59.724	13090
Focusing quadrupole 1 (FQ1)	1295	36	46.62	10874
Focusing quadrupole 2 (FQ2)	1295	47	60.865	10874
Defocusing quadrupole (DQ)	1295	83	107.485	10874

cables in the region of Ω run horizontally, while the straight section of the other pair is vertical. Such arrangement minimises the interactions between the bus-bars.

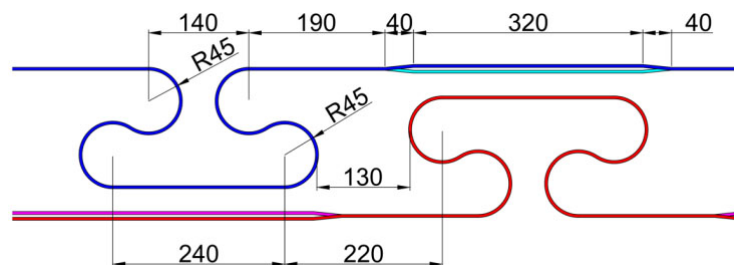


Fig. 2. Dimensions of Ω -shaped dilatations

To find the size of the induced currents one has to consider the mutual inductances and the self-inductances of the elements of the circuit. Figure 3 shows the diagram of coupling between two current lines. L_M denotes the self-inductance of a magnet supplied with a current by a line, L_L is the self-inductance of the line, U_C is the voltage inducing a current and U_P is the voltage powering the magnet. The numbers represent the respective lines.

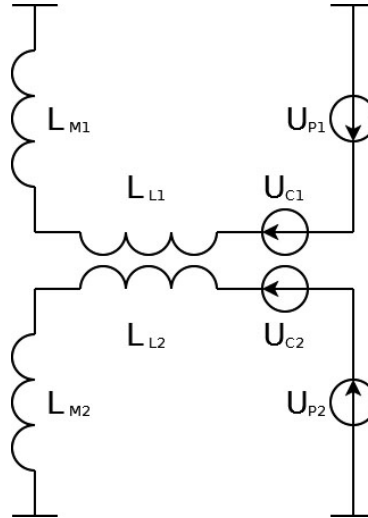


Fig. 3. Simplified diagram of a coupling between two current lines

The basic formulas of circuit theory will be used in further analysis. Formula (1) shows the relation between the time-varying current I , inductance L and induced voltage U .

$$I = \frac{1}{L} \int U dt. \tag{1}$$

The induced voltage U_{Cnm} induced at the line n by the current I_m at the line m , is found with Formula (2). M_{mn} denotes the mutual inductance between the lines.

$$U_{Cnm} = M_{mn} \frac{dI_m}{dt}. \tag{2}$$

Using these formulas the induced current I_{Cn} can be calculated using Formula (3).

$$I_{Cn} = \frac{1}{L_{Mn} + L_{Ln}} \int U_{Cn} dt = \frac{1}{L_{Mn} + L_{Ln}} \int M_{mn} \frac{dI_m}{dt} dt. \tag{3}$$

This formula can be further transformed into (4).

$$I_{Cn} = \frac{M_{mn}}{L_{Mn} + L_{Ln}} I_m = \frac{M_{mn}}{L_{Mn} + L_{Ln}} \cdot \frac{1}{L_{Mm} + L_{Lm}} \int U_{Pm} dt. \tag{4}$$

To find the total value of the induced currents all possible couplings between the lines have to be considered. The scheme of mutual inductances and their markings are presented in Figure 4.

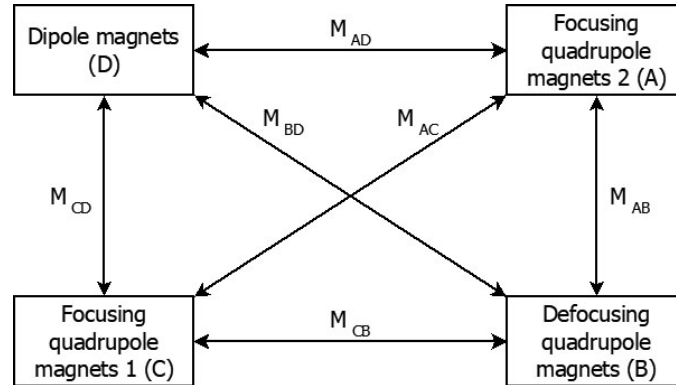


Fig. 4. Mutual inductances between the lines

2.2. Numerical calculations

Numerical calculations are performed using Comsol's AC/DC package and checked with QuickField. The self-inductance of a single pair of the superconducting cables per unit length is found as a function of the distance between the axes of the cables l_c . The geometry of the bus-bar allows varying the distance in the range of 9 to 20 mm. In this case simple 2D geometry and DC currents are applied. The numerical meshes used in the models are presented in Figure 5.

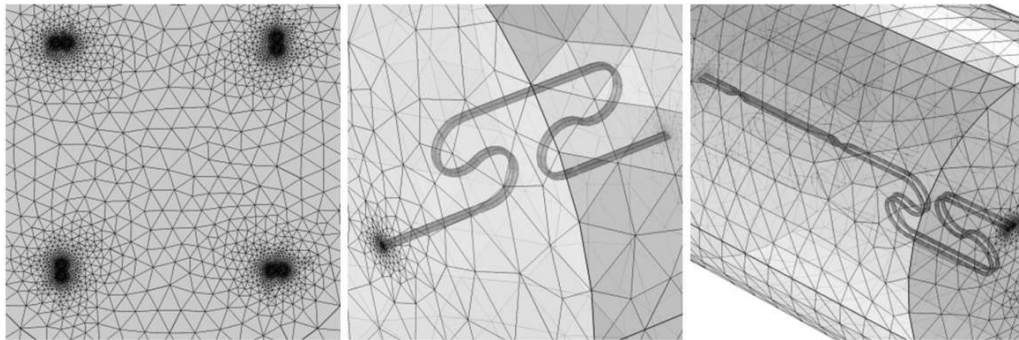


Fig. 5. Numerical meshes applied in the models (left to right – 2D model for the calculation of line inductances, 3D model for the calculation of self-inductance of a dilatation, 3D model for the calculation of the mutual inductances in a dilatation region)

Two numerical methods are used to find self-inductance. The first is based on the calculation of a magnetic flux. Self-inductance can be defined with Formula (5) as the ratio between the magnetic flux Ψ generated by and penetrating a circuit, generated by the current I flowing through it.

$$L = \frac{\Psi}{I}. \quad (5)$$

To calculate Ψ the magnetic vector potential A is integrated over the cross-section of the cable S_c according to Formula (6).

$$\Psi = \frac{\iint_{S_c} A dx dy}{S_c}. \quad (6)$$

To find the self-inductance of the return circuit the mutual effects of the cables have to be considered. The final formula used during the calculations is the following (7):

$$L = \frac{\Psi_1 - \Psi_2}{S_c I}. \quad (7)$$

Suffix numbers denote each cable in a pair.

An alternative approach is based on the calculation of the magnetic energy W , generated by the electric current flow through the circuit. It is found by the integration of magnetic energy density w over the entire model region Φ (Formula (8)).

$$W = \int_{\Phi} w d\Phi. \quad (8)$$

w is calculated with Formula (9).

$$w = \frac{1}{2} [(B_x + B_y) \cdot H_x + (B_x + B_y) \cdot H_y]. \quad (9)$$

After finding the total magnetic energy, self-inductance can be found with Formula (10).

$$L = \frac{2W}{I^2}. \quad (10)$$

Due to the simplicity of geometry an analytical formula for self-inductance of two parallel wires with uniform currents exists (Formula (11)) [8]. In the formula r denotes the radius of the cable, μ_0 is the magnetic permeability of vacuum.

$$L = \frac{\mu_0}{\pi} \left[\ln \left(\frac{l_c}{r} \right) + \frac{1}{4} \right]. \quad (11)$$

Mutual inductance of a line per unit length M_l is found using the magnetic flux method and an induced voltage method. The magnetic flux method is applied similarly to the calculation of self-inductance. The main difference is the placement of the electric current. For the calculation of the mutual inductance per unit length M_{lAB} between lines A and B , Formula (12) is applied.

$$M_{lAB} = \frac{\Psi_{B1} - \Psi_{B2}}{S_c I_A}. \quad (12)$$

To find M using the voltage method the AC currents with the frequency of 1 Hz are applied in selected cables. This frequency is similar to the one applied during the training regime of the accelerator as well as some of the normal operation modes. The operation of the accelerator is described in greater detail in [6]. The condition of homogeneous current density is applied.

On the cables other than the current-carrying ones the condition of zero current is used. Then the difference between voltages V induced in the cables of each pair is found. Mutual inductance is calculated with Formula (13). In this formula ω is the pulsation of the current I_A .

$$M_{IAB} = \frac{V_{B1} - V_{B2}}{I_A \omega i}. \quad (13)$$

Self-inductance in a dilatation region is calculated using a 3D model with DC currents. The entire geometry of the dilatation is recreated, as shown in Figure 5. The creation of optimal mesh for such geometry poses certain challenges. In order to shorten the time of calculations the elements along straight sections are elongated by a factor of 10. The mesh in the region where the cables are bent is very dense to account for all nuisances of the shape of the magnetic field. The characteristic size of elements is approximately 2 mm.

In the remaining region the mesh is coarser. The shortest computation times are observed when the region of cables is placed in the centre of a cylindrical environment with radius 2.5 times larger than the largest vertical dimension of the dilatation. In given conditions it is approximately 500 mm with a characteristic element size of 80 mm.

In the calculations of self-inductance of dilatation the energy method is used. The obtained result is given in H. During the calculation of the total self-inductance the obtained value has to be multiplied by the number of dilatations in the entire line. In the case of a single section the total value of self-inductance is found with Formula (14).

$$L_t = L_l \cdot (l_l - l_d) + L_d. \quad (14)$$

L_t is here the total self-inductance of a section, L_l is the line self-inductance, l_l is the length of the section, l_d is the length of the modelled dilatation region and L_d is the calculated inductance of the dilatation region.

The calculation of mutual inductance in the dilatation region is performed using a 3D model of the entire assembly with the dimensions according to Figure 2. During the calculations of mutual inductance between the two lines only one of them is modelled as a 3D object. The other is assumed to be a linear current and modelled as such. The condition of a single turn coil is imposed on the 3D line region. Ground and current source conditions are used on opposite ends of the cable, where it intersects the external surface of the environment region.

The mesh is complex and prone to errors, especially close to the twist of the cables. In their vicinity, the characteristic size of the mesh element is 0.5 mm. In the remaining cable region it is 1–2 mm, depending on the bending of the line. The environment has a similar radius as in the case of self-inductance calculation. However, the mesh is roughly twice as dense. The general view of the mesh is presented in Figure 5. Because of the complexity of the mesh this part of calculations is the longest.

Mathematically, the voltage method is applied in the same way as it was done in a 2D model. Mutual inductance is given in H. Formula (15) used to calculate the mutual inductance of a single section is analogical to (14).

$$M_t = M_l \cdot (M_l - M_d) + M_d. \quad (15)$$

M_t is here the total mutual inductance of a section, M_l is the line mutual inductance, l_l is the length of the section, l_d is the length of the modelled dilatation region (including two dilatations

and the region in which interactions are expected to occur) and M_d is mutual inductance of the dilatation region found with the numerical model.

3. Results and discussion

Figure 6 shows the dependence of the line self-inductance of a straight section of the transfer line on the distance between the cables. Three calculation methods yield practically the same results, and the values show the expected logarithmic dependence. Self-inductance increases from 424 nH/m (when the separation is 9 mm) to 743 nH/m (separation of 20 mm). The obtained results are comparable with the experimental results described in [9]. A smaller system was measured and the obtained values of the line inductance for a single cable were ranging from 260.6 nH/m to 281.4 nH/m for the distance between cables close to 11 mm.

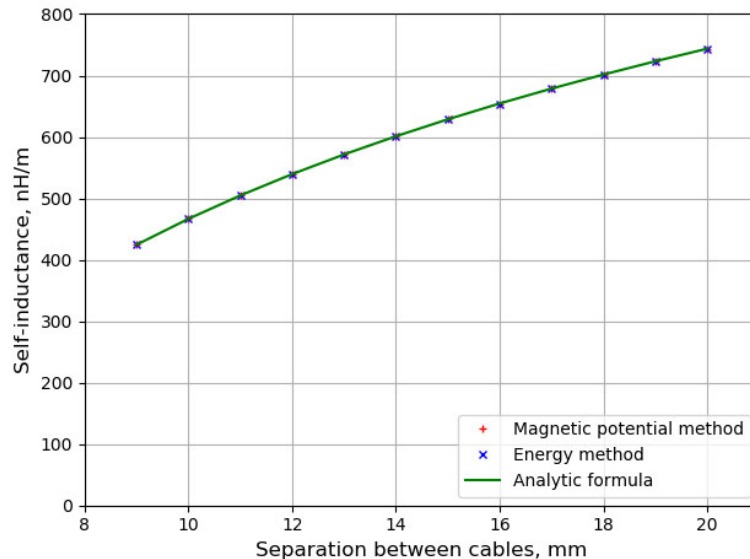


Fig. 6. Line self-inductance of the straight sections of the line

The dependence of line mutual inductance of a straight section on the distance between the cables is presented in Figure 7. Both methods yield the same results again. An induced voltage method is observed to give accurate results in lower densities mesh. Thus, it is less time-consuming. The dependence between the values has a different character. The inductance is proportional to the square of the distance between the cables. The values of M_{AD} , M_{CB} , M_{CD} and M_{AB} are very close to each other and significantly smaller than M_{BD} and M_{AC} . This is because in the first cases the planes of the lines are perpendicular to each other. In such setting the magnetic field generated by both cables affecting the second pair is mostly compensated. When the planes are parallel the linking flux is significantly higher and strongly increases with the decreasing distance between the pairs, as seen in the comparison between M_{AC} and M_{BD} .

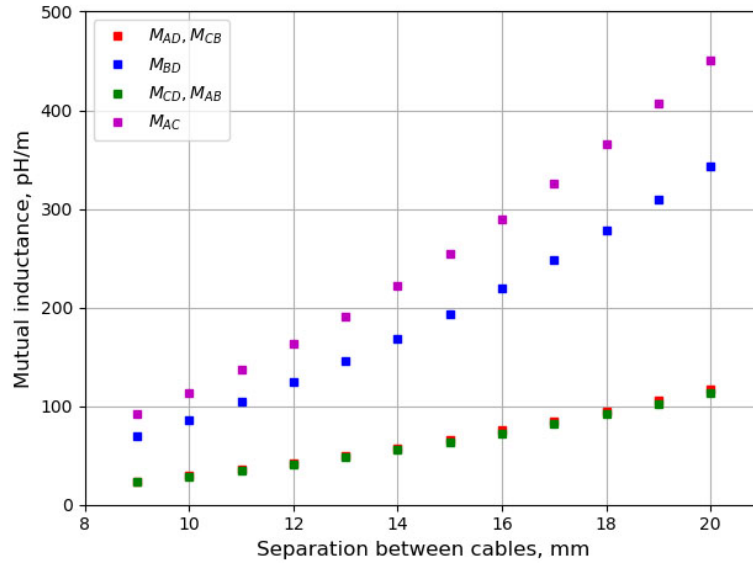


Fig. 7. Line mutual inductances of the straight sections of the line

Dependence of the self-inductance of a dilatation on the distance between the cables is shown in Figure 8. The logarithmic dependence is visible, similarly to line inductance. The self-inductance of the dilatation is 2.4–2.5 times higher than of a straight section with the same length. This difference decreases with the distance between the cables.

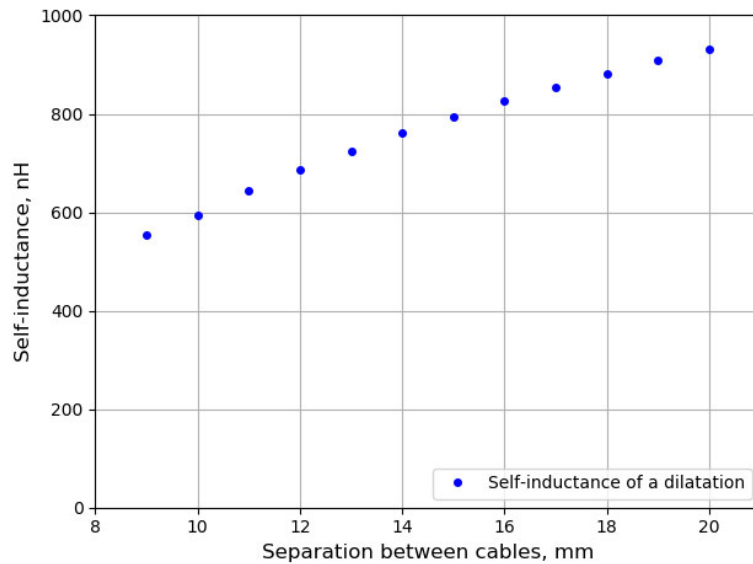


Fig. 8. Self-inductance of a dilatation

The total self-inductance of all sections as a function of the distance between the cables is shown in Figure 9. The logarithmic dependence is still visible. The value increases from 122 μH for a distance of 9 mm and 213 μH at 20 mm.

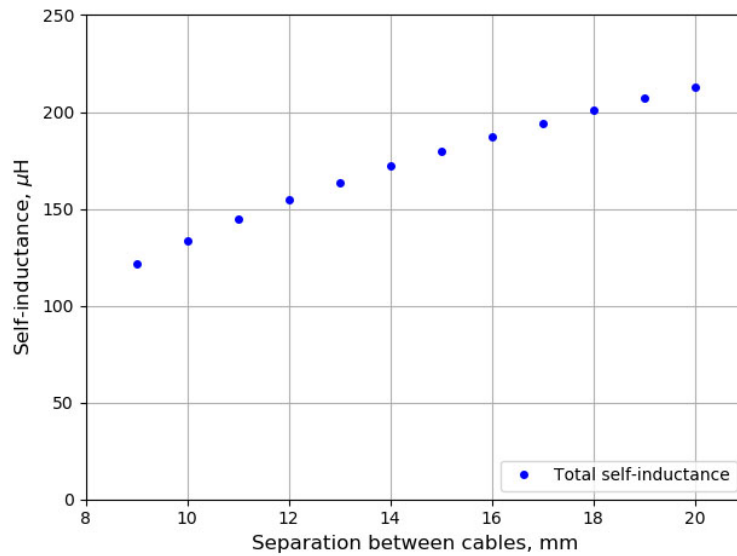


Fig. 9. Total self-inductance of by-pass lines

Figure 10 shows the values of mutual inductances in a dilatation region in dependence on the distance between the cables. It can be seen that, while most of the inductances have similar

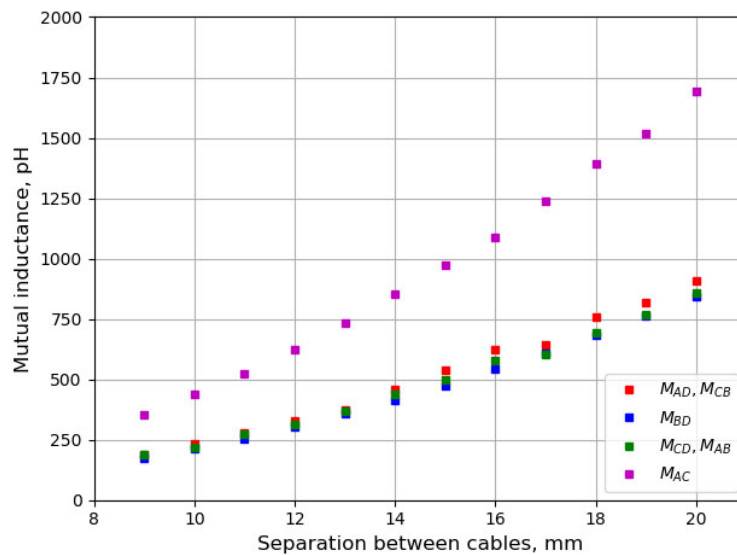


Fig. 10. Mutual inductances in dilatation regions

values, M_{AC} is significantly higher. The interaction between two lines for quadruple magnets is stronger because of the geometry of the line. In this case long regions where the lines lie on parallel planes exist. Additionally, they are relatively close to each other. The mutual inductances of the dilations differ strongly from the analogical straight sections. It is from 2.5 (for M_{BD}) up to 8 (for M_{AD} and M_{CB}) times larger in dilatation region.

Figure 11 shows the expected maximum values of induced currents. It can be seen that square dependence observed in the mutual inductance values dominates over logarithmic dependence of the self-inductance. The values of the currents are similar in each line except for dipoles. In this case it is lower. This is due to the fact that the current in the dipole line is higher than in the rest and causes stronger disturbances in the remaining lines.

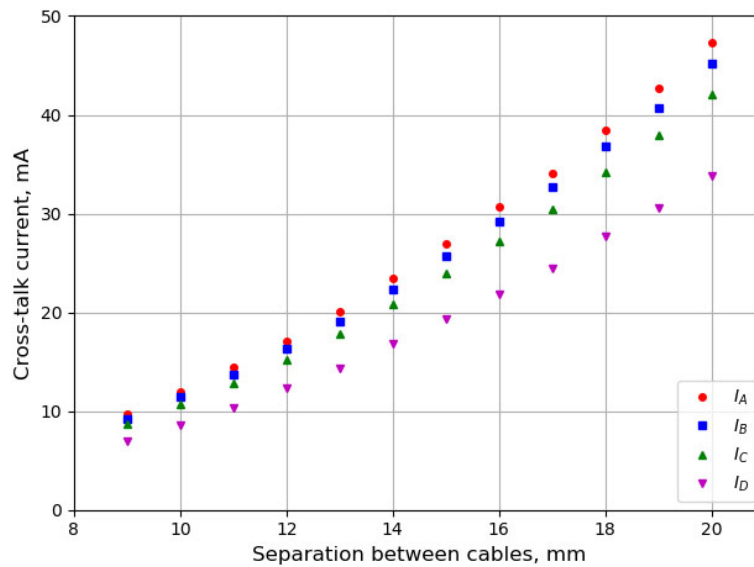


Fig. 11. Maximum induced currents

The size of the induced currents decreases with the distance between the cables in each line. Therefore, it should be maintained as low as possible from the construction point of view. The discrepancy of currents translates in the worst case to a magnetic field variation of approximately 7.7 μT . The decrease of the distance to 9 mm allows for obtaining a discrepancy of 1.2 μT .

4. Conclusion

The values of self-inductances and mutual inductances are found using numerical calculations. Based on these values the induced currents and the magnetic discrepancy connected with them are calculated. The results obtained with different calculation methods are consistent. The magnetic field discrepancy falls in the range of 1.2 μT to 7.7 μT . The results for small distances fall well within the required operational limit for the electromagnets, which is 6.25 μT . Therefore, placing

the cables close to each other in a bus-bar allows the reliable operation of the accelerator. Further changes in the design would be possible to decrease the induced currents, such as slight increase of distance between bus-bars.

The dependence of self-inductance on the distance between the cables is logarithmic. The mutual inductance is proportional to square of this distance. Square dependence seems to dominate in the calculations of an induced current and it quickly increases with the distance between the cables in the bus-bar. Therefore, it should be as small as possible. In the final design the distance is 9.5 mm, close to a minimum of 9 mm.

Acknowledgements

This work has received funding from Ministry for Science and Higher Education under FAIR in-kind Contract between Facility for Antiproton and Ion Research in Europe GmbH, Jagiellonian University and Wrocław University of Science and Technology. The authors are grateful to Wrocław Networking and Supercomputing Centre for granting access to the computing infrastructure.

References

- [1] Outeiro M.T., Visintini R., Buja G., *Considerations in designing power supplies for particle accelerators*, IECON 2013 – 39th Annual Conference of the IEEE, Industrial Electronics Society, pp. 7076–7081 (2013).
- [2] Bertarelli A., *Beam-induced damage mechanisms and their calculation*, CERN Yellow Reports, vol. 2, pp. 159–227 (2016).
- [3] Kauschke M., Xiang Y., Schroeder C.H., Streicher B., Kollmus H., *Cryogenic supply for accelerators and experiments at FAIR*, American Institute of Physics Conference Proceedings, vol. 1573, iss. 1, pp. 1200–1205 (2014).
- [4] Kahle K., *Power Converters and Power Quality*, Proceedings of the CAS-CERN Accelerator School: Power Converters (2015).
- [5] Eisel T., Chorowski M., Iluk A., Kauschke M., Kollmus H., Malcher K., Poliński J., Streicher B., *Local Cryogenics for the SIS100 at FAIR*, IOP Conference Series: Materials Science and Engineering, vol. 101 (2015), DOI: 10.1088/1757-899X/101/1/012075.
- [6] Trojanowski S., Cizek M., Chorowski M., *Calculations and measurements of cross-talks in simulated and optimized current lines supplying magnets of SIS-100 accelerator with Ω -shaped dilatation loops*, in Polish: *Obliczenia i pomiary przesłuchów w symulowanych i optymalizowanych liniach prądowych zasilających magnesy akceleratora SIS100, z pętlami dylatacyjnymi w kształcie „omeg”*, Wrocław University of Technology (unpublished) (2016).
- [7] Tomków Ł., Trojanowski S., Cizek M., Chorowski M., *Analysis of capacitance of a cryogenic by-pass line for SIS100 particle accelerator at FAIR*, Archives of Electrical Engineering, vol. 67, no. 4 (2018).
- [8] Tomków Ł., Trojanowski S., Cizek M., Chorowski M., *Heat generation by eddy currents in a shell of superconducting bus-bars for SIS100 particle accelerator at FAIR*, Archives of Electrical Engineering, vol. 66, no. 4, pp. 705–715 (2017).
- [9] Claycomb J., *Applied Electromagnetics Using QuickField and Matlab*, Jones and Bartlett Publishers, Boston (2010).
- [10] Trojanowski S., Cizek M., Chorowski M., *Measurements of capacitances and self-inductances of lines supplying superconducting magnets (project FAIR)*, in Polish: *Pomiary pojemności oraz indukcyjności własnych w liniach zasilających magnesy nadprzewodnikowe (projekt FAIR)*, Wrocław University of Technology (unpublished) (2015).